The menaquinone pathway is important for susceptibility of *Staphylococcus aureus* to the antibiotic adjuvant, cannabidiol

Claes Søndergaard Wassmann [a], Andreas Pryds Rolsted [a], Mie Cecilie Lyngsie [a], Sergi Torres-Puig [a], Tina Kronborg [a], Martin Vestergaard [b], Hanne Ingmer [b], Steen Plesner Pontoppidan [c], Janne Kudsk Klitgaard [a,d,*]

[a] *Department of Biochemistry and Molecular Biology, Research Unit of Molecular Microbiology, University of Southern Denmark, Denmark*
[b] *Department of Veterinary and Animal Sciences, Faculty of Health and Medical Sciences, University of Copenhagen, Denmark*
[c] *Canna Therapeutic ApS, Denmark*
[d] *Institute of Clinical Research, Research Unit of Clinical Microbiology, University of Southern Denmark, Denmark*

ARTICLE INFO

ABSTRACT

Emergence of antibiotic resistant bacteria is evolving at an alarming pace; therefore, we must start turning to alternative approaches. One of these, could be the use of antibiotic adjuvants that enhances the effect of antibiotics towards resistant bacteria. A novel antibiotic adjuvant is cannabidiol (CBD), which we have previously shown can enhance the effect of bacitracin (BAC). BAC targets cell wall synthesis by inhibiting dephosphorylation of the lipid carrier undecaprenyl pyrophosphate prior to recycling across the membrane. However, the mechanism underlying this CBD mediated potentiation of BAC has remained unknown. To explore this, we examined resistance to CBD in *Staphylococcus aureus* through daily exposures to CBD. By subsequent whole genome sequencing, we observed multiple genes to be mutated, including the *farE/farR* system encoding a fatty acid efflux pump (FarE) and its regulator (FarR). Importantly, recreation of mutations in these genes showed decreased susceptibility towards the combination of CBD and BAC. Furthermore, we searched the Nebraska Transposon Mutant Library for CBD susceptible strains and identified *menH* encoding a protein participating in menaquinone biosynthesis. Strains containing deletions in this and other menaquinone related genes showed increased susceptibility towards CBD, while addition of exogenous menaquinone reversed the effect and reduced susceptible towards CBD. These results suggest that CBD potentiates BAC by redirecting the isoprenoid precursor isopentenyl pyrophosphate towards production of menaquinone rather than the lipid carrier undecaprenyl pyrophosphate, which dephosphorylation is inhibited by BAC. This in turn might decrease the level of undecaprenyl pyrophosphate thus enhancing the effect of BAC. Our study illustrates how antibiotic adjuvants may apply to enhance efficacy of antimicrobial compounds.

1. Introduction

The excessive use of antibiotics has led to rapid emergence of antimicrobial resistance as a global issue. The antibiotic resistance development exhibits a correlation with the amount of antibiotics used, and the multidrug-resistant pathogens are developing and spreading at an alarming pace (Aslam et al., 2018). Infections with multidrug-resistant pathogens are more difficult to treat, and both the length and the cost of the hospitalization, as well as the fatality rate and morbidity, increases (Bin Zaman et al., 2017; Medina and Pieper, 2016). One of the pathogens known to cause complex nosocomial infections is the

Gram-positive bacterium *Staphylococcus aureus*. *S. aureus* is often resistant towards a variety of antimicrobials such as a broad range of β-lactams including methicillin (Methicillin-Resistant *S. aureus*, MRSA) (Gurung et al., 2020). In worst cases, MRSA also possesses resistance towards last-resort antibiotics such as vancomycin and daptomycin (Lowy, 2003; Sievert et al., 2008). With the restricted repertoire of antibiotics against MRSA and other multidrug-resistant pathogens, it is important to find alternative treatment strategies such as use of antibiotic adjuvants. Antibiotic adjuvants, also known as resistance breakers (Laws et al., 2019) and helper compounds (Martins et al., 2008), increase the effect of an antibiotic towards a bacterium that otherwise

might be resistant towards that specific antibiotic (Douafer et al., 2019). A classic example of an antibiotic adjuvant used in the clinic is the beta-lactamase inhibitor clavulanic acid that enhances the effect of amoxicillin by preventing degradation by beta-lactamases (Douafer et al., 2019). However, to date very few antibiotic adjuvants are used in the clinic (Douafer et al., 2019).

Cannabidiol (CBD), the main non-psychoactive ingredient of the *Cannabis sativa* plant, has antimicrobial affects against a variety of bacteria (Appendino et al., 2008; Van Klingeren and Ten Ham, 1976) and a documented bactericidal activity against MRSA (Blaskovich et al., 2021). We have previously shown that CBD, acts as an antibiotic adjuvant in combination with the antibiotic bacitracin (BAC) (Wassmann et al., 2020). BAC interferes with cell wall synthesis by binding to the important lipid carrier undecaprenyl pyrophosphate (UPP). This interaction prevents the undecaprenyl pyrophosphate phosphatase (UppP) mediated dephosphorylation of the lipid carrier thus preventing recycling and further polymerization of the peptidoglycan and forcing *de novo* synthesis of UPP by the undecaprenyl pyrophosphate synthase (UppS) (Hiron et al., 2011; Shaaly et al., 2013). *De novo* synthesis of UPP requires production of the isoprenoid precursor isopentenyl pyrophosphate (IPP) by the mevalonate pathway, which is then converted to farnesyl pyrophosphate (FPP) an isoprenoid also used for synthesis of the carotenoid staphyloxanthin and the vital electron transporter menaquinone (Balibar et al., 2009).

In our previous study, we showed that CBD lowered the minimum inhibitory concentration (MIC) of BAC by up to at least 64-fold and showed to have great antimicrobial effects on its own against several Gram-positive bacteria. In addition, we found that the combination of CBD and BAC resulted in morphological changes indicated by several septa formation and membrane irregularities in MRSA resulting in severe cell division defects. Furthermore, we observed that CBD itself was able to disrupt the membrane potential of *S. aureus* (Wassmann et al., 2020).

In the present study, we seek to understand the underlying mechanism of CBD and the CBD mediated potentiation of BAC through various approaches. These include generation of CBD resistant strains, transcriptomic analysis by RNA sequencing upon treatment with CBD, BAC, and the combination and by screening the Nebraska Transposon Mutant Library (NTML) for CBD susceptible strains.

2. Methods and materials

2.1. Bacteria and growth conditions

Staphylococcus aureus USA300 FPR3757 (Diep et al., 2006) (addressed as USA300), was the main bacterium used throughout this study. USA300 was grown in Mueller Hinton (MH) (Merck) or Brain Heart Infusion (BHI) (OXOID) media on plate or in liquid cultures.

2.2. Mutant frequency determination

Log-phase bacteria at a concentration of 10^6–10^{10} CFU/mL were plated onto MH agar plates containing CBD at a concentration of 4 x MIC, and the plates were incubated at 37 °C for 48 h. In addition, 10-fold dilutions of each culture were plated on drug-free media to provide accurate colony counts. Mutant frequency was calculated by dividing the number of colonies growing on antibiotic plates by the total number of CFU plated. The experiment was performed in biological triplicates, and mutant frequency represent an average value. To verify the stability of each resistant bacteria, they were transferred several times in drug-free medium and medium containing CBD at 4 x MIC and were again tested for resistance.

2.3. Selection of CBD resistant strains by in vitro serial passaging

CBD resistant USA300 was generated by serial passaging growing USA300 in daily increasing concentration of CBD (Merck) and was performed as described by Ling and colleagues (Ling et al., 2015). An overnight (ON) culture of USA300 was diluted 1:100 in MH media in five separate tubes supplemented with increasing concentrations of CBD (0.2, 0.4, 0.6, 0.8, and 1.0 µg/mL CBD). The cultures were incubated at 37 °C with agitation and passaged at 24 h intervals in the presence of CBD at subinhibitory concentration. In practice, OD_{600} was measured and the culture with the second highest concentration of CBD allowing $OD_{600} > 2$ was chosen for further passaging, diluting the culture 1:100 in MH media containing higher concentrations of CBD. The experiment was performed for a total of 14 days with creation of freeze stocks each day. Cultures collected were streaked on MH plates and a single colony was selected for storage to ensure homogenous culture.

2.4. DNA sequencing and mutational analysis

DNA sequencing of the resistant strains as well as the wildtype USA300 was performed by use of the Illumina MiSeq platform with paired end 150 bp reads. The wildtype strain was sequenced as well to rule out putative single-nucleotide polymorphisms previously present in the genome, thus enabling identification of unique mutations acquired by the CBD resistant strains. Library preparation was performed by use of the Nextera XT DNA Kit (Illumina). The Whole Genome Sequencing (WGS) data were analysed using the Breseq pipeline from Barrick Lab (Deatherage and Barrick, 2014) aligning the WGS data to the reference genome of *S. aureus* USA300 FPR3757 (NC_007793) and subsequently analysing for mutations using the COMPARE tool. The analysis was performed using the Ubuntu operation system. Mutations were verified by PCR using the check_F/R primers and followed by sequencing at EurofinsGenomics. Full list of primers (Merck) used in this study can be found in Supplementary A.

2.5. CBD susceptibility testing of the Nebraska Transposon Mutant Library

Susceptibility of the Nebraska Transposon Mutant Library (NTML) (Fey et al., 2013) was tested against CBD (THC Pharm). The NTML distributed on twenty 96-well plates was spotted on twenty MH plates containing 1 µg/mL CBD and 5 µg/mL erythromycin (since the transposon used to create the library contains the resistance cassette *ermB*) using a Duetz 96 cryo-replicator. The cryo-replicator was sterilized by submerging the pins in 96 % ethanol (EtOH) followed by ignition with fire. The plates were incubated at 37 °C ON and growth was assessed as growth or no growth.

2.6. Creation of gene deletion and site directed mutagenesis mutants

In-frame deletion of selected genes (*atpD*, *tarO*, *farE*, *farR*, *menH*, *hepT*, *menA* and *ispA*) as well as creation of strains containing site directed mutagenesis (SDM) mutations (*walR*$_{A453C}$, *atpD*$_{T421A}$, *tarO*$_{C710A}$, *farE*$_{T1750A}$, *farR*$_{G280T}$ and *far*$_{G80/86A}$) were achieved through splicing by overlap extension PCR according to Monk and colleagues (Monk et al., 2012). Specific primers utilized for creation of deletion and SDM mutants are listed in Supplementary A. For creation of gene deletion mutants, fragments of 500 bp up and down-stream of the gene of interest was amplified using Phusion polymerase (Thermo Fisher Scientific) and joined by overhang PCR. For creation of SDM mutants, an approximate 500 bp sequence up and down-stream of the site of the desired mutation was amplified. The reverse primer for the up-stream fragment and the forward primer for the down-stream fragment were reverse complement to each other and contained the desired mutation. The inserts and vector pIMAY were digested with *Sal*I (Thermo Fisher Scientific) and/or *Sac*I at 37 °C and ligated using T4 DNA Ligase (Roche) at 16 °C. pIMAY containing the insert of interest were transformed into CaCl₂ chemically competent *Escherichia coli* IM08B, purified by GenElute Plasmid Miniprep Kit (Merck) and transformed into electrocompetent *S. aureus*

USA300 created by 0.5 M sucrose wash. Colonies grown on BHI plates containing 20 μg/mL chloramphenicol (CHL) were identified as positive transformants by colony PCR using primers IM151 and IM152 (Monk et al., 2012). Positive transformants were incubated on BHI agar containing 20 μg/mL CHL at 28 °C. Genomic integration of the plasmid was achieved by inoculating ON culture in BHI containing 20 μg/mL CHL followed by incubation at 37 °C. Plasmid integration was verified by PCR using primers primer D + outF and primer A + outR for the respective gene. Plasmid excision was carried out by daily dilution of ON culture in BHI media with incubation at 28 °C for approximately 7 days. The culture was plated on BHI containing 1 μg/mL anhydrotetracycline (AHT) for counter selection and incubated at 28 °C for 1–2 days. Colonies were subsequently spotted on BHI agar with and without 20 μg/mL CHL followed by incubation ON at 37 °C. Colony PCR was performed for CHL sensitive colonies verifying gene deletion using the the outF and outR primers. Mutant creation was verified by sequencing at Eurofins Genomics using the outF + outR primers for gene deletion or SDM_check_F and SDM_check_R primers for SDM mutants.

2.7. Minimum inhibitory concentration (MIC) determination

MIC was determined using the broth microdilution method (Wiegand et al., 2008). Briefly, MIC measurements were performed using MH or BHI medium in 96-well plates (Sarstedt). A bacterial inoculum of approximately 5×10^5 CFU/mL from either an ON culture or from a plate was incubated with two-fold dilution series of the compound of interest. The plates were incubated at 37 °C for 16–22 h with agitation. MIC determinations were performed using at least three biological replicates. Growth was determined using a Synergy H1 Plate Reader (BioTek).

2.8. Growth experiments

Growth experiments in 96-well plates were performed by use of Synergy H1 Plate reader. Plates and bacterial cultures were prepared as mentioned above. Growth experiments were performed for 24 h at 37 °C with continuous agitation measuring OD_{600} every 1 h. Experiments were performed in at least three biological replicates.

Growth experiments in flasks were performed as well. An ON culture of USA300 was diluted to $OD_{600} = 0.02$ in MH media and incubated at 37 °C until early exponential phase at $OD_{600} = 0.2$. Cells were split into separate flasks and treated with either CBD, BAC (Merck) or the combination of CBD + BAC or left untreated. Menaquinone-4 (MK-4) (Merck) was added in respective flasks as well. Experiments were performed in three biological replicates.

2.9. Creation of pRAB12-farE for inducible expression

For inducible expression of *farE*, the vector pRAb12-lacZ (Helle et al., 2011) was used. The vector was digested with *Bgl*II and *Eco*RI at 37 °C to remove *lacZ*. Since *Eco*RI restriction site is present in the *farE* gene, a multiple cloning site (MCS) was inserted with the primers Fwd_pRAB12_MCS_Overhang and Rev_pRAB12_MCS_Overhang creating the vector pRAB12-MCS. pRAB12-MCS, as well as the *farE* insert created by PCR using primers Up_*farE*_BglI and Dw_*farE*_NotI, were digested with *Bgl*II and *Not*I. Digested pRAB12-MCS and *farE* insert were ligated using T4 DNA Ligase (Roche) at 16 °C ON and transformed into competent *E. coli* IM08B. The plasmid was purified from IM08B using GenElute Plasmid Miniprep Kit (Merck), transformed into electrocompetent USA300 and plated on BHI agar containing 20 μg/mL CHL. Positive transformants were verified using the primers pRAB12_Seq_F and pRAB12_Seq_R.

2.10. RNA purification and qRT-PCR

ON cultures of USA300 + pRAB12-farE and USA300 + pRAB12-MCS

grown in BHI containing 20 μg/mL CHL were diluted to an $OD_{600} = 0.02$ and grown for 4 h at 37 °C in BHI media with and without addition of 100 ng/mL AHT to induce *farE* expression. Cells were harvested by centrifugation. RNA was extracted by a hot acid-phenol procedure, pelleted on ice, washed in 70 % EtOH and finally resuspended in sterile ddH_2O. 1 μg of purified RNA was treated with DNase I (NEB) at 37 °C for 15 min and then heat inactivated at 75 °C for 10 min. cDNA synthesis was carried out using the High-Capacity cDNA Reverse Transcriptase Kit (Thermo Fisher Scientific) and performed as recommended by the manufacturer. RT-qPCR was performed on the cDNA samples using 2x RealQ Plus Master Mix Green (Ampliqon) and primers (Supplementary A) in a LightCycler 480 instrument (Roche). The house keeping gene *gyrB* was used for normalization. Reactions were carried out using the following procedure: 15 min preincubation at 95 °C, followed by 45 amplification cycles at 95 °C for 15 s, 60 °C for 45 s and 72 °C for 45 s. Data was retrieved using the LightCycler 480 Software. Experiment was performed in four biological replicates.

2.11. RNA-sequencing and analysis

ON cultures of wildtype USA300 were diluted in BHI media till $OD_{600} = 0.02$ and grown at 37 °C with agitation till $OD_{600} = 0.2$. Cells were exposed to either 1 μg/mL CBD, 16 μg/mL BAC, combination of CBD and BAC or left untreated for 20 min at 37 °C with agitation. Cells were quickly cooled using liquid nitrogen and harvested by centrifugation. RNA purification was performed as mentioned above. rRNA was removed by use of Ribo-Zero rRNA Removal Kit for bacteria (Illumina), and was performed according to manufacturer's recommendation. Library preparation was performed using the NEBNext RNA Library preparation kit (New England BioLabs) followed by quality assessment using a fragment analyzer. Sequencing was performed using an Illumina HiSeq 1500. Data analysis was performed using Bowtie2 (Langmead and Salzberg, 2012) in the local mode. Sequences were indexed and sorted using SAMtools and reads were counted in featureCounts (Liao et al., 2014). Counts matrix was submitted to the R/Bioconductor package DESeq2 for statistical analysis (Love et al., 2014). Fold-change values were size-estimated using the apeglm package (Zhu et al., 2018). Data were sorted by log2 fold-change and statistical significance was set at *p* value < 0.05. Expression of selected candidate genes identified in the RNA-seq analysis was validated using RT-qPCR in three biological replicates, as previously described (Supplementary E).

2.12. Carotenoid quantification

Carotenoid extraction and quantification was carried out according to (Kossakowska-Zwierucho et al., 2016) and (Sen et al., 2016) with adjustments. Briefly, ON culture of USA300 was diluted in BHI and grown at 37 °C from $OD_{600} = 0.02$ to $OD_{600} = 0.2$ and treated with either 1 μg/mL CBD, 16 μg/mL BAC, combination of CBD and BAC, EtOH control or left untreated for 4 h at 37 °C with agitation. Cells were harvested corresponding to $OD_{600} = 2.0$ in 5 mL and washed twice in sterile ddH_2O. Pellet was resuspended in 1.5 mL 99 % methanol and incubated at 55 °C with agitation cycles of 1 min agitation followed by 10 s of no agitation for 10 min. 100 μL sample was used for OD_{600} measurement for normalization of data due to potential variance in bacterial amount. Samples were centrifuged at 10,000xG for 15 min and 1 mL of the supernatant was measured spectrophotometrically at OD_{465}. Experiment was performed in three biological replicates.

3. Results

3.1. Creation and characterization of CBD resistant USA300 mutants

To understand the antimicrobial activity of CBD, we generated CBD resistant strains to reveal indications of the antimicrobial mechanism of CBD. When investigating the mutant frequency of single-step

spontaneous mutations on plates containing 4 x MIC (16 (µg/mL)) of CBD, only a few *S. aureus* mutants could be found. Hence, the resistance frequency of single-step resistance-generating mutations was 1.4×10^{-8}, indicating a single drug target within the cell (O'Neill and Chopra, 2004).

Furthermore, we examined the emergence of resistance to CBD by creating CBD resistant strains through exposure of *S. aureus* USA300 to daily increasing concentrations of CBD in liquid MH media for 14 days. MIC for CBD was subsequently assessed for the individual isolates collected at day 4, 6, 7, 8, 10, 11, 12 and 14 (called CBD4, CBD6, CBD7, CBD8, CBD10, CBD11, CBD12 and CBD14) and showed decreased susceptibility towards CBD ranging from 4 µg/mL for the wildtype strain and CBD4 to 128 µg/mL or more for CBD14 (Table 1).

To study the putative mutations possibly causing adaptation to CBD, the genome of the CBD resistant strains was sequenced. From the mutational analysis, we found multiple genes to be mutated (Table 2) all resulting in a missense mutation. CBD8−14 contained a A453C mutation in *walR*, encoding a response regulator of the two-component system WalRK (Dubrac et al., 2007). A T421A mutation was observed in *atpD* of CBD7, encoding a beta-subunit of the ATP synthase (Bosch et al., 2020). CBD14 contained a C710A mutation in *tarO*, encoding an enzyme of the wall teichoic acid biosynthesis (Suzuki et al., 2012). CBD8−14 contained a T1750A mutation *farE* and CBD4−12 contained a G280 T mutation in *farR*, encoding a fatty acid efflux pump (FarE) and its regulator (FarR) (Alnaseri et al., 2015), respectively. Furthermore, a mutation (G80/86A) was observed in the intergenic region between *farE* and *farR*.

3.2. Phenotypical analysis of observed genes mutated in CBD resistant strains

In order to characterize the influence of each individual mutation on the susceptibility towards CBD, we created individual strains in wildtype USA300 containing the point mutations as well as creating gene deletion mutants of affected genes, with exception of the *walR* as it is essential for growth *in vitro* (Dubrac et al., 2007; Zheng et al., 2015). MIC for CBD was determined on created mutants (Table 3). Interestingly, results showed unaltered MIC of the different mutants for CBD compared to the wild-type strain, indicating that multiple mutations might be required simultaneously in order to gain resistance towards CBD.

Next, we performed growth experiments using the mutants exposing with both CBD, BAC, and the combination. Growth experiments showed that at a combination of 2 µg/mL CBD and 32 µg/mL BAC the wildtype strain was unable to initiate growth (Fig. 1A), while some of the generated mutants were able to grow. One of these, USA300*farR*$_{G280T}$ (Fig. 1F), showed an extended lag-phase of 15 h but reverting to an OD$_{600}$ close to that of the untreated cells after 24 h. An initiation of growth was also observed for USA300*walR*$_{A543}$ (Fig. 1B) and USA300-*farE*$_{A1750T}$ (Fig. 1E) when exposed to the combination of 2 µg/mL CBD and 32 µg/mL BAC, though not as pronounced as the one observed in USA300*farR*$_{G280T}$. The remaining mutants did not initiate growth during the 24 h when exposed to the combination treatment.

Table 1
MIC for CBD of CBD resistant strains created by serial passage experiment.

CBD Resistant Strain	MIC CBD (µg/mL)
WT USA300	4
CBD4	4
CBD6	8
CBD7	8
CBD8	16
CBD10	16
CBD11	16
CBD12	32
CBD14	≥128

As both USA300*farR*$_{G280T}$ and USA300*farE*$_{A1750T}$ showed decreased susceptibility towards the combination of CBD and BAC compared to the wildtype and as we did not observe any changes regarding the susceptibility towards CBD alone, we created a double mutant containing both *farR*$_{G280T}$ and *farE*$_{A1750T}$ mutations (USA300*farE*$_{T1750A}$*farR*$_{G280T}$) and also one containing both *farR*$_{G280T}$ and *far*$_{G80/86A}$ (USA300-*farR*$_{G280T}$*far*$_{G80/86A}$). Interestingly, MIC for CBD increased by two-fold in USA300*farE*$_{T1750A}$*farR*$_{G280T}$ at 8 µg/mL while USA300*farR*$_{G280T}$*far*$_{G80/86A}$ still showed an MIC at 4 µg/mL (Table 3). Furthermore, comparing the growth of these mutants with that of the USA300*farR*$_{G280T}$ strain upon treatment with the combination, it did not seem to be significantly different (Fig. 1L and 1 M). Therefore, our results might suggest a possible role of FarE and FarR in CBD susceptibility. To investigate this further we therefore created an *farE* inducible plasmid. We amplified the *farE* gene and placed it downstream of an anhydrotetracycline (AHT) inducible promoter creating pRAB12-*farE*. Induced expression was verified by RT-qPCR (Supplementary B1), showing an approximately 14-fold increased expression for pRAB12-*farE* upon addition of the inducer AHT, compared to the empty plasmid (pRAB12-MCS). Surprisingly, no differences were observed for USA300/pRAB12-*farE* regarding CBD susceptibility (Supplementary B2) or susceptibility towards the combination of CBD and BAC (Fig. 1N) compared to the strain carrying the empty plasmid USA300/pRAB12-MCS (Fig. 1O) questioning the role of *farE* and *farR* regarding CBD susceptibility. Another explanation could be that the level of induced expression is not sufficient to affect CBD susceptibility.

3.3. Transcriptional response to CBD, BAC, and the combination

Since creation of CBD resistant strains did not provide us with a clear explanation regarding the mechanism of action of CBD and how it potentiates the effect of BAC, we examined the transcriptional changes upon treatment with CBD, BAC, and the combination. Cells were grown to early exponential phase and treated for 20 min to observe the initial response to the compounds which showed remarkable changes in the global gene expression (Fig. 2). Genes with statistically significant expressional changes and with ≥1 Log2 fold change (Log2FC) are listed in Supplementary C. Interestingly, expression of *farE* (Fig. 2A) was observed to be the third most upregulated gene upon CBD treatment, further suggesting its potential role in CBD susceptibility and thus the importance of the mutations mentioned above in relation to the effect of CBD. Other noticeable genes are *hrtA* and *hrtB* (Fig. 2A) encoding a heme transporter (Stauff et al., 2008), being the second and the first most upregulated genes upon CBD treatment, respectively. Upon BAC treatment, we observed that *vraD* and *vraE*, which encode proteins of the VraDE bacitracin transporter (Hiron et al., 2011), were the two most upregulated genes (Fig. 2B).

To further analyse and get a deeper understanding of the RNA-seq data, we performed GO Term Enrichment Analysis using DAVID (Huang da et al., 2009; Huang et al., 2009; Mi et al., 2020) (Supplementary D). Interestingly, pathway enrichment analysis upon combination treatment showed enrichment of genes participating in terpenoid backbone biosynthesis, also known as the mevalonate pathway (Supplementary D4). These genes include *mvaD*, *mvaK1*, and *mvaK2* (Fig. 2C).

3.4. Carotenoid quantification of S. aureus upon treatment

Since the mevalonate pathway showed to be enriched in the transcriptional analysis during combination treatment, we thought to investigate this further. As suggested by Balibar and colleagues, when the amount of IPP is limited the downstream application is redirected towards essential pathways such as production of UPP for peptidoglycan biosynthesis (Balibar et al., 2009). This means that activity in non-essential pathways such as production of the carotenoid staphyloxanthin will be decreased. We therefore thought to study the effect of

Table 2
Mutations observed by whole-genome sequencing of the CBD resistant strains.

Gene/Area Affected	Locus Tag	Mutation	Amino Acid Change	Protein Function [a]	CBD Resistant Strain
walR	SAUSA300_0020	A453C	K151N (AA$\underline{A}$→AA$\underline{C}$)	Sensor Histidine Kinase	CBD8, CBD10, CBD11, CBD12 and CBD14
atpD	SAUSA300_2058	T421A	L141I (T$\underline{T}$A→A$\underline{T}$A)	ATP Synthase Subunit Beta	CBD7
tarO	SAUSA300_0731	C710A	P237Q (C$\underline{C}$A→C$\underline{A}$A)	Glycosyl transferase group 4 family protein	CBD14
farE	SAUSA300_2489	T1750A	I584F (A$\underline{T}$T→$\underline{T}$TT)	Antibiotic transport-associated protein-like	CBD8, CBD10, CBD11, CBD12 and CBD14
farR	SAUSA300_2490	G280T	D94Y (G$\underline{A}$T→T$\underline{A}$T)	Regulator protein, TetR family	CBD4, CBD6, CBD7, CBD8, CBD10, CBD11 and CBD12
farE/farR		G80/86A			CBD12

[a] Protein function retrieved from https://www.uniprot.org/.

Table 3
MIC for CBD of created mutants.

Strains	MIC CBD (µg/mL)
WT USA300	4
USA300*walR*$_{A453C}$	4
USA300*atpD*$_{T421A}$	4
USA300*tarO*$_{C710A}$	4
USA300*farE*$_{T1750A}$	4
USA300*farR*$_{G280T}$	4
USA300*far*$_{G80/86A}$	4
USA300Δ*atpD*	4
USA300Δ*tarO*	4
USA300Δ*farE*	4
USA300Δ*farR*	4
USA300*farE*$_{T1750A}$*farR*$_{G280T}$	8
USA300*farR*$_{G280T}$*far*$_{G80/86A}$	4

treatment with CBD, BAC, and the combination on the production of the carotenoid staphyloxanthin. Interestingly, the level of carotenoid production was not only reduced by combination treatment (3-fold reduction) (Fig. 3), CBD treatment also caused a lower level of carotenoids (2-fold reduction), suggesting that CBD somehow influences the use of IPP.

3.5. Screening of the Nebraska Transposon Mutant Library for CBD susceptible mutants

A third approach we investigated was to search the Nebraska Transposon Mutant Library (NTML) for CBD susceptible transposon mutants. The NTML created by the Nebraska Center for Staphylococcal Research consist of 1952 single gene disruption mutants in the CA-MRSA strain USA300 JE2 (Fey et al., 2013). The NTML was spotted on MH plates containing 1 µg/mL CBD and incubated ON at 37 °C. CBD susceptible strains (Table 4) were identified by lack of growth. To verify increased susceptibility of identified transposon mutants, a MIC determination was performed. Surprisingly, MIC showed that only a few of the identified strains that did not grow on CBD containing plates had an MIC below that of the wildtype (WT). These included strains with disruption of the genes SAUSA300_0847, *menH*, *fur*, and *hemB*. Some strains did not show a consistent MIC value, since it ranged from 2 to 4 µg/mL compared to the wildtype MIC at 4 µg/mL. However, only *menH* was chosen for further studies due to its vital role in the menaquinone biosynthesis (Vitamin K2) (Dawson et al., 2011), a metabolic pathway which also requires IPP.

3.6. Menaquinone decreases susceptibility towards cannabidiol

To study the influence of menaquinone production upon susceptibility towards CBD, we created an in-frame deletion mutant of *menH*, including other genes contributing to menaquinone biosynthesis (*hepT*,

menA, and *ispA*). MIC of CBD was determined on all four mutants and showed a two-fold decreased MIC value at 2 µg/mL for all of them (Table 5), compared to the WT. Since fitness of USA300Δ*hepT* and USA300Δ*menA* was highly reduced, the experiments using these strains were performed in the nutrient rich medium BHI. Wildtype USA300 was grown in both MH and BHI media. We thought to test susceptibility towards BAC as well and results showed a two-fold increased MIC for both USA300Δ*hepT* and USA300Δ*ispA* at 256 and 128 µg/mL, respectively, compared to the wildtype USA300 having an MIC for BAC at 64 µg/mL in MH medium and 128 µg/mL in BHI medium. Since deletion of the genes participating in the menaquinone pathway resulted in increased susceptibility towards CBD, we investigated the effect of exogenous menaquinone. Interestingly, by addition of 50 µM (22.2 mg/mL) menaquinone-4 (MK-4) wildtype USA300 became less susceptible towards CBD (Table 5) indicated by a four-fold increased MIC value at 16 µg/mL. A similar effect also observed for the other deletion mutants (Table 5), suggesting that presence of menaquinone can somehow prevent the damaging effects of CBD. Furthermore, we performed a growth experiment using CBD at concentrations of 1, 4 and 8 µg/mL with and without addition of 50 µM MK-4 (Fig. 4A). Importantly, cells that received 4 and 8 µg/mL CBD showed initial and similar growth to that of the untreated cells when exogenous MK-4 was added as well, whereas cells that only received 4 and 8 µg/mL CBD, and not MK-4, showed no or very reduced growth. We also performed the experiment with the combination of CBD and BAC which interestingly showed that MK-4 was also able to prevent the CBD-mediated potentiation of BAC (Fig. 4B). Next, we tested if addition of higher concentration of MK-4 was able to decrease the effectiveness of CBD even further. By addition of 500 µM MK-4 (Fig. 4C), USA300 was able to grow in concentrations as high as 64 µg/mL CBD. In general, growth in presence of CBD showed to be dependent on MK-4 concentration. Furthermore, we investigated whether this altered susceptibility caused by exogenous MK-4 was specific for CBD only. Interestingly, altered susceptibility was not observed upon treatment with other antibiotics such as bacitracin, vancomycin, chloramphenicol, ciprofloxacin or daptomycin (Table 6), suggesting that this effect is specific for CBD. Finally, we studied how USA300 responded to CBD in presence of 1,4-dihydroxy-2-naphthoic acid (DHNA), an intermediate molecule of the menaquinone pathway used by MenA (Choi et al., 2017). DHNA has been observed to be an allosteric inhibitor of MenD in *Mycobacterium tuberculosis* (Bashiri et al., 2020) causing decreased menaquinone production. If this is also applicable for *S. aureus*, one could expect an opposite effect regarding MK-4 addition.. By addition of 50 µM DHNA (10.2 mg/mL), USA300 became more susceptible towards CBD indicated by almost no growth at 0.5 µg/mL CBD compared to the cells that did not receive DHNA, suggesting that DHNA could be an allosteric inhibitor of Staphylococcal MenD as well (Fig. 4D). These data supports that the effects of CBD on the membrane of *S. aureus* can be counteracted by presence of menaquinone.
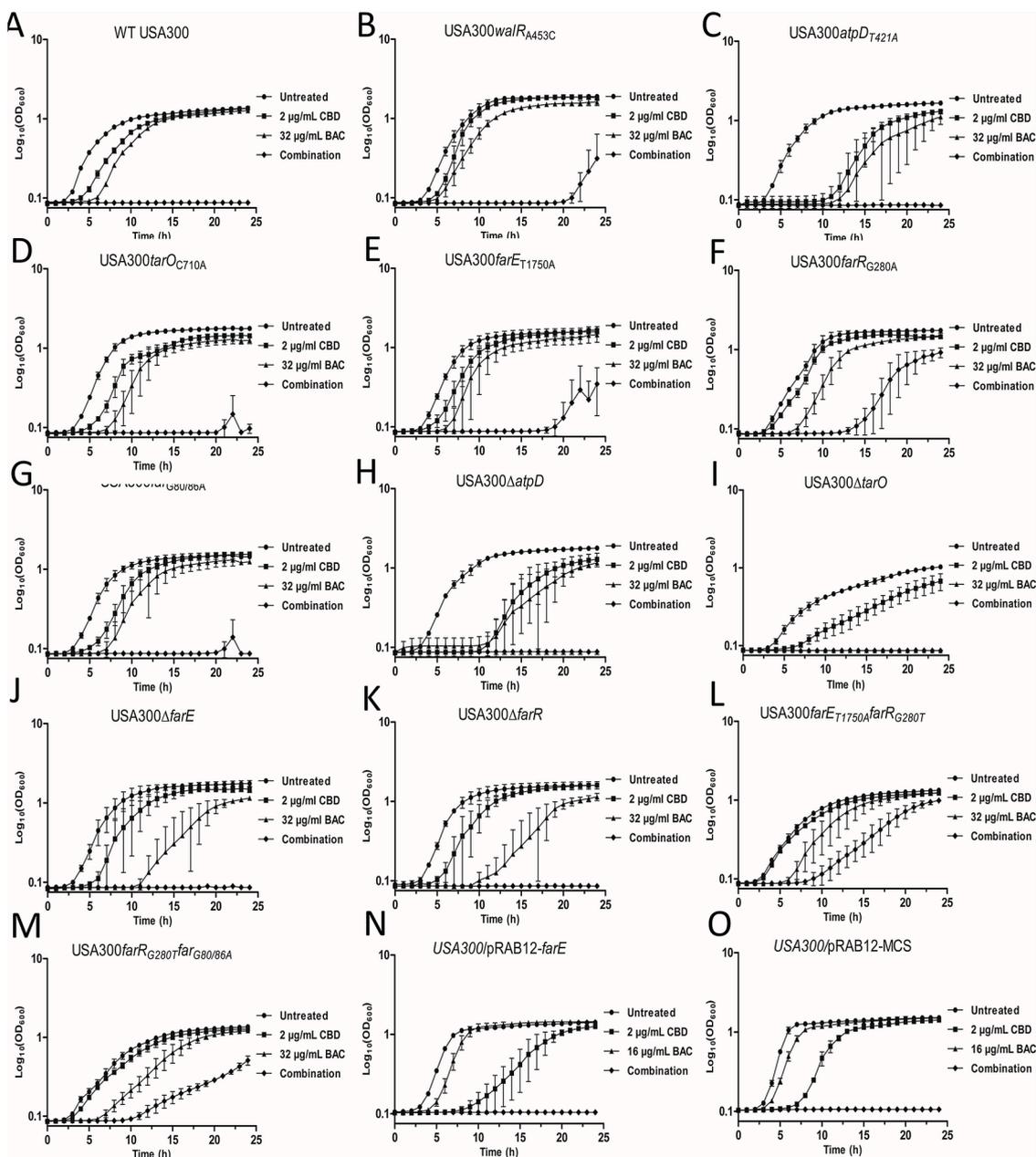
Fig. 1. Growth experiments of WT USA300 (A), created mutants (B-M) and USA300 with inducible plasmid pRAB12-*farE* (N) and empty plasmid pRAB12-MCS (O) treated with either CBD (■), BAC (▲), combination (◆) or left untreated (●).

4. Discussion

In previous work, we discovered the use of the cannabinoid CBD as a novel antibiotic adjuvant able to potentiate the effect of the antibiotic BAC against Gram-positive bacteria such as *Staphylococcus aureus, Listeria monocytogenes,* and *Enterococcus faecalis* (Wassmann et al., 2020). However, the mechanism underlying the CBD mediated potentiation of BAC remains unknown. We therefore investigated this.

The mutant frequency to antibacterial resistance indicates a single drug target within the cell. However, selection of CBD resistant strains and subsequent whole genome sequencing identified multiple mutated genes. These included *walR, atpD, tarO, farE,* and *farR* as well as a mutation in the intergenic region between *farE* and *farR*.

Mutations in the *farER* system were observed in all CBD resistant strains. *farE* (fatty acid resistance effector) encodes a resistance-nodulation-division efflux pump shown to promote resistance towards linoleic and arachidonic acids in *S. aureus* (Alnaseri et al., 2015). *farE*

expression is regulated by FarR (fatty acid resistance regulator), a member of the TetR family of transcriptional regulators (Alnaseri et al., 2019). Recreation of the mutations observed in the *farER* system (*farE*$_{T1750A}$ and *farR*$_{G280T}$) did not show altered CBD susceptibility; however, it resulted in a decreased susceptibility towards the combination of CBD and BAC. Especially for USA300*farR*$_{G280T}$, susceptibility towards the combination of CBD and BAC seemed significantly decreased when compared to the wildtype strain. Additionally, susceptibility did not change for the strain containing the *far*$_{G80/86A}$ mutation or for the gene deletion mutants of both *farE* and *farR* compared to the wildtype strain. We furthermore created a strain containing two mutations, USA300*farE*$_{T1750A}$*farR*$_{G280T}$ showed a two-fold increased CBD MIC value of 8 μg/mL, whereas USA300*farR*$_{G280T}$*far*$_{G80/86A}$ did not yield an MIC value different from that of the wildtype. These results indicate a potential role for FarE and FarR in CBD susceptibility and CBD mediated potentiation of BAC. Mutations in *farR* resulting in decreased susceptibility towards certain antimicrobials has been observed before. Nguyen
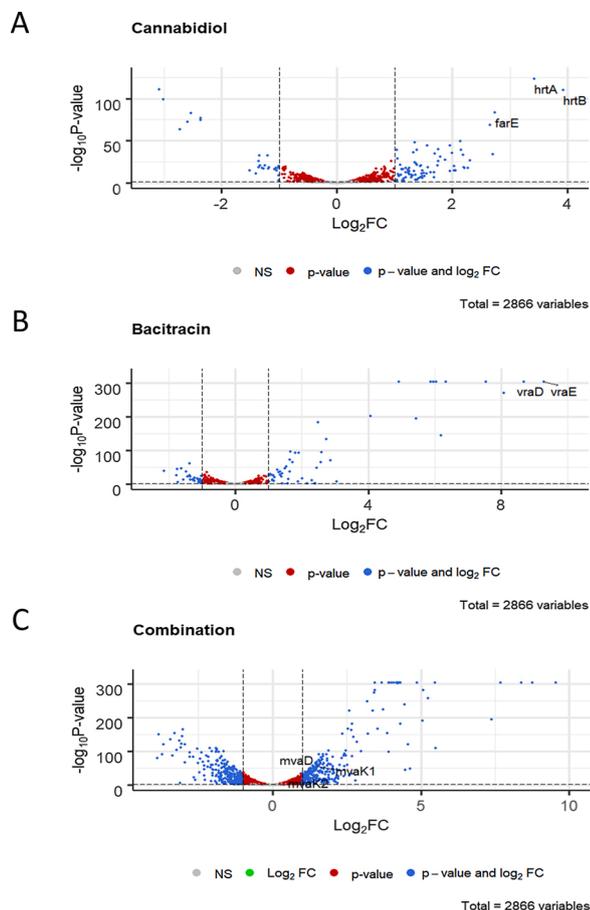
A

Cannabidiol

B

Bacitracin

C

Combination

Fig. 2. Volcano plots of the transcriptional expression of USA300 upon treatment with CBD (A), BAC (B) and the combination (C) compared to untreated cells.
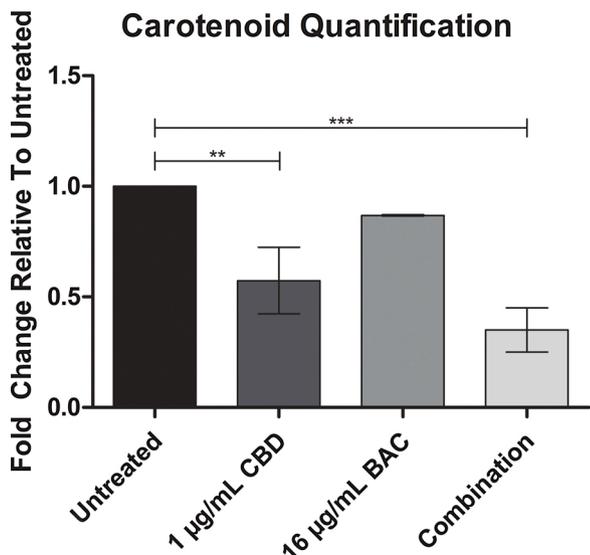
Carotenoid Quantification

Fig. 3. Carotenoid quantification of USA300 upon treatment with CBD, BAC or the combination relative to untreated. Statistics were performed using one-way ANOVA with Bonferroni correction.

and colleagues showed that a point mutation in *farR* causing an amino acid substitution from Cys to Arg at position 116 resulted in decreased susceptibility towards rhodomyrtone, an acylphloroglucinol antimicrobial isolated from the plant *Rhodomyrtus tomentosa* (Nguyen et al.,

Table 4
CBD susceptible strains observed in the screening of the Nebraska Transposon Mutant Library as well as MIC for CBD of these..

Gene Name	Locus Tag	Protein Function	MIC (µg/mL)
	SAUSA300_0199	Conserved hypothetical protein	4
	SAUSA300_0377	Putative lipoprotein	4
cydD	SAUSA300_0670	ABC transporter ATP-binding protein	2–4
cydC	SAUSA300_0671	ABC transporter ATP-binding protein	2–4
	SAUSA300_0847	Thioesterase	2
menH	SAUSA300_0947	Hydrolase, alpha/beta hydrolase fold family	2
qoxC	SAUSA300_0961	Quinol oxidase, subunit III	2–4
qoxB	SAUSA300_0962	Quinol oxidase, subunit I	2–4
purK	SAUSA300_0967	Phosphoribosylaminoimidazole carboxylase, ATPase subunit	4
purF	SAUSA300_0972	Amidophosphoribosyltransferase	4
ctaM	SAUSA300_1017	Hypothetical protein	2–4
	SAUSA300_1182	Pyruvate ferredoxin oxidoreductase, alpha subunit	4
	SAUSA300_1183	2-oxoglutarate ferredoxin oxidoreductase subunit beta	4
bshA	SAUSA300_1349	Glycosyl transferase, group 1 family protein	4
fur	SAUSA300_1514	Ferric uptake regulation protein	2
mtnN	SAUSA300_1558	5'-methylthioadenosine/S-adenosylhomocysteine nucleosidase	2–4
cymR	SAUSA300_1583	Hypothetical protein	2–4
hemB	SAUSA300_1615	Delta-aminolevulinic acid dehydratase	2

Table 5
MIC for CBD with and without addition of menaquinone-4 (MK-4) and MIC for BAC of mutants.

Strain	MIC CBD (µg/mL)	MIC CBD + 50µM MK-4	MIC BAC (µg/mL)
WT USA300	4	16	64
WT USA300 (BHI)	4	16	128
USA300Δ*menH*	2	8	64
USA300Δ*hepT*	2	16	256
USA300Δ*menA*	2	16	128
USA300Δ*ispA*	2	8	128

2019). They also observed an increased release of lipids and fatty acids from the strain containing the *farR* mutations, suggesting that release of these might result in binding and inactivation of rhodomyrtone (Nguyen et al., 2019), a mechanism of antimicrobial resistance also observed for daptomycin (Pader et al., 2016). In another case, Chen and colleagues discovered a point mutation in *S. aureus* SH1000 resulting in the exact same amino acid substitution as discovered in our CBD resistant strains, FarR$_{D94Y}$, as discovered in our CBD resistant strains, causing decreased susceptibility towards D-sphingosine, an unsaturated long chain amino alcohol found on the human skin (Chen et al., 2020). These observations further emphasize the potential role of FarE and FarR regarding CBD susceptibility. Unfortunately, overexpression of *farE* did not result in altered susceptibility towards CBD or the combination of CBD and BAC. However, this could be explained by insufficient FarE expression levels to alter susceptibility to CBD. Nevertheless, recreating the *farR*$_{G280T}$ mutation in a wildtype strain did in fact show a decreased susceptibility towards the combination of CBD and BAC indicating that the FarE/FarR system might have a potential role, among others, in the mechanism of resistance towards CBD. Furthermore, the RNA-seq data showed *farE* to be the third most upregulated gene upon CBD treatment, highlighting its potential role regarding CBD susceptibility, perhaps through release of fatty acids and/or lipids binding and inactivating CBD. As suggested by Nguyen and colleagues, FarR might be regulating expression of multiple genes both directly and indirectly (Nguyen et al., 2019), indicating that the *farR* mutation observed causing decreased susceptibility towards the combination of CBD and BAC could be caused by altered expression of
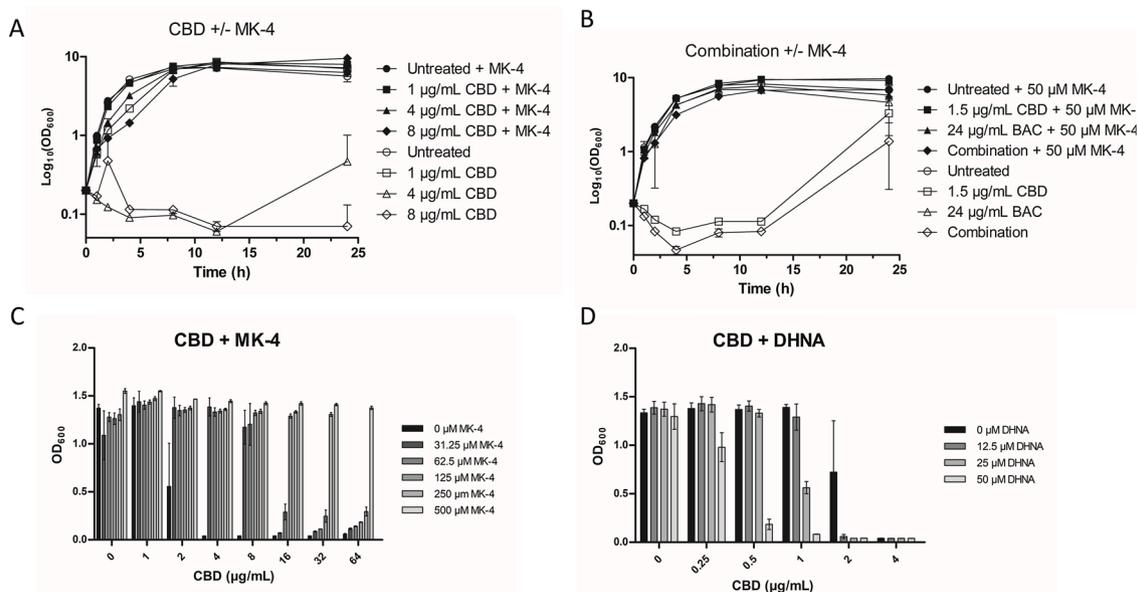
Fig. 4. Growth experiments with and without addition of menaquinone-4 (MK-4) in the presence of CBD (A) and combination of CBD and BAC (B). Susceptibility test of CBD with increasing concentrations of MK-4 (C) and 1,4-dihydroxy-2-naphthoic acid (DHNA) (D), against USA300. Untreated + MK-4 (●), CBD + MK-4 (■), BAC + MK-4 (▲), Combination + MK-4 (◆), Untreated (○), CBD (□), BAC (△) and Combination (◇).

Table 6
MIC determination of USA300 for multiple antimicrobials with and without addition of 50 μM menaquinone-4 (MK-4).

Compound	MIC (μg/mL) ÷ MK-4	MIC (μg/mL) + MK-4
Cannabidiol	4	16
Bacitracin	64	64
Vancomycin	0.5	0.5
Chloramphenicol	16	16
Ciprofloxacin	8	8
Daptomycin	16	16

additional FarR regulated genes and not *farE* expression alone.

USA300*walR*_{A543C} also showed decreased susceptibility towards the combination of CBD and BAC. *walR* encodes a transcriptional regulator that, together with WalK form the essential two component system WalRK (Dubrac et al., 2007; Ji et al., 2016). WalRK has shown to be important for regulation of various cellular processes such as autolysis (Dubrac et al., 2007), production of biofilm, cell wall metabolism and regulation of virulence genes through SaeSR activation (Delauné et al., 2012). These important processes in *S. aureus* might be slightly dysregulated in USA300*walR*_{A543C}, however, since only minor changes had occurred in the mutants regarding CBD and BAC susceptibility, the consequence of the mutation might be limited. Mutations in *walRK* have been associated with reduced susceptibility towards other antimicrobials such as daptomycin (Friedman et al., 2006; Yin et al., 2019) and vancomycin (Howden et al., 2011; Hu et al., 2016), both targeting the cell envelope, also a potential target for CBD (Blaskovich et al., 2021; Wassmann et al., 2020), suggesting a potential role for the two component system in regards to CBD susceptibility. The *walR* mutation was indeed observed in multiple CBD resistant strains including the highly CBD resistant strain CBD14. Beside this, CBD14 is the only strain also containing a mutation in *tarO* encoding an enzyme responsible for the first step in the biosynthesis of wall teichoic acid (WTA) in *S. aureus* (Suzuki et al., 2012). WTAs are long glycopolymers found in the cell wall of Gram-positive bacteria (van Dalen et al., 2020). WTA has shown to be important for maintaining the rigidity and charge of the cell envelope and regulate permeability (Suzuki et al., 2011) as well as protecting the cell against environmental stress such as host skin fatty acids (Kohler

et al., 2009), high temperature (Vergara-Irigaray et al., 2008) and antimicrobials such as vancomycin (Peschel et al., 2000) and human antimicrobial peptides (Collins et al., 2002) due to alanylation of the WTA. This emphasizes its potential contribution to the high MIC value of CBD observed in CBD14. In addition to this, as mentioned for WalRK, WTA has also been observed to be important for regulation of autolysis (Schlag et al., 2010). Dysregulated autolysis has been associated with altered susceptibility towards various antibiotics such as vancomycin (Boyle-Vavra et al., 2003; Meehl et al., 2007) and daptomycin (Patel et al., 2011), indicating that the mutation observed in both *walR* and *tarO* together might contribute to, at least in some degree, the highly CBD resistant phenotype of CBD14.

Secondly, we screened the NTML for genes relevant to CBD susceptibility. The NTML enables a high-throughput screening of almost all non-essential genes in *S. aureus* and has been used to identify genes important for susceptibility towards various anti-staphylococcal antimicrobials (Vestergaard et al., 2016), polymyxins (Vestergaard et al., 2017), salt resistance (Schuster et al., 2020) and genes important for virulence during silkworm infection (Paudel et al., 2020). Importantly, we found that the NTML mutant *menH*, which has a disrupted menaquinone pathway (vitamin K₂) (Dawson et al., 2011), showed increased susceptibility towards CBD. Further investigations showed that strains with deletion of other genes participating in menaquinone biosynthesis (*menA*, *hepT*, and *ispA*), also showed increased susceptibility towards CBD, whereas some of the strains also showed decreased susceptibility towards BAC. Interestingly, growing *S. aureus* in presence of 50 μM MK-4 allowed for growth in above MIC concentration of CBD (MIC at 16 μg/mL), a tendency that seems to be concentration-dependent since growth in even higher concentrations of MK-4 (500 μM) resulted in growth of *S. aureus* at 64 μg/mL CBD. This effect showed to be specific for CBD only, since combining MK-4 with other antimicrobials did not result in altered susceptibility towards these.

Menaquinone is an essential part of the electron transport chains during respiration as it helps transporting electrons between electron acceptors along the bacterial membrane (Kurosu and Begari, 2010; Truglio et al., 2003). This facilitates proton movement across the membrane thus creating the transmembrane proton gradient (ΔpH) that together with the membrane potential (Δψ) generate the proton motive force (PMF) that drives ATP synthesis (Farha et al., 2013; Kurosu and Begari, 2010). Disruption of the Δψ will lead to an increase in ΔpH and

vice versa enabling maintenance of the PMF (Bakker and Mangerich, 1981; Farha et al., 2013). This means that *S. aureus* might attempt to compensate the membrane potential disruptive effects of CBD, which has been previously shown (Wassmann et al., 2020) (Blaskovich et al., 2021), by increasing the transmembrane proton gradient, ΔpH, through increased levels of menaquinone. Supporting this hypothesis, we furthermore observed an opposite effect when combining CBD with DHNA, an intermediate of the menaquinone pathway. DHNA has been discovered in *Mycobacterium tuberculosis* to be a negative allosteric regulator of MenD, the first committed step in menaquinone biosynthesis (Bashiri et al., 2020). If this is also applied for *S. aureus* it could further emphasize that presence of menaquinone disrupts the effect of CBD, since presence of a menaquinone biosynthesis inhibitor, in this case DHNA, makes *S. aureus* more susceptible towards CBD.

The fact that presence of CBD might lead to increased menaquinone production could also explain the decreased carotenoid production observed when exposed to CBD. IPP and FPP are key metabolites in production of staphyloxanthin, UPP, and menaquinone, hence, presence of CBD might cause redirection of IPP and FPP for production of menaquinone rather than staphyloxanthin and UPP. This could also explain how CBD enhances the effect of BAC. It is evident from the RNA-seq data that *S. aureus* might attempt to compensate the increased IPP and FPP demand caused by the combination of CBD and BAC by upregulating the mevalonate pathway (terpenoid backbone pathway) when exposed to the combination. However, since synergy is observed for CBD and BAC, the putative increased IPP and FPP production might not be sufficient.

To further support the idea that menaquinone counteracts the effect of CBD by increasing the transmembrane proton gradient, we discovered three additional transposon mutants in the NTML screen showing increased CBD susceptibility. One of these, SAUSA300_0847, encodes a protein that has sequence similarity with MenI, the enzyme in the menaquinone pathway that creates DHNA in other bacteria, such as *E. coli*. In addition, we observed that the two most upregulated genes upon CBD treatment encode the HrtAB transporter that transports heme (Stauff et al., 2008), a cofactor also used during respiration by terminal oxidases for reduction of O_2 to H_2O (Hammer et al., 2013). Two strains

with disruption in one of these oxidases, *qoxB* and *qoxC*, encoded on the *qoxABCD* operon (Hammer et al., 2013), was also identified in our NTML screen to be more sensitive towards CBD. The fact that the strain containing disruption of *hemB*, required for heme biosynthesis, was also observed to be CBD sensitive might rather be due to the small colony forming unit phenotype of this strain (Mike et al., 2013). An NTML screen was also performed by Farha and colleagues (Farha et al., 2020) using cannabigerol, another cannabinoid from *Cannabis sativa*. Transposon strains with disruption of genes participating in menaquinone biosynthesis were not identified in their screen. However, *aroC* (SAUSA300_1357), encoding the final enzyme of the chorismate biosynthesis, a precursor for menaquinone biosynthesis (Zhang et al., 2017), was found to be sensitive towards cannabigerol when disrupted, emphasizing the potential role of menaquinone biosynthesis in sensitivity towards CBD and perhaps also other cannabinoids.

Based on the result obtained from the NTML screen and further analysis we propose a model of which CBD enhances the effect of bacitracin (Fig. 5). As previously published (Wassmann et al., 2020), we observed that CBD was able to disrupt membrane potential through a yet still unknown mechanism. We speculate that, in order to maintain the PMF and thus ATP production, *S. aureus* increases the production of menaquinone that in turn will increase the transmembrane proton gradient. Therefore, *S. aureus* shifts the use of IPP and FPP towards menaquinone and thus decreases the production of UPP and staphyloxanthin. As the UPP production is decreased the effect of BAC is therefore potentiated due to inhibition of UPP recycling by BAC and synthesis by CBD, leading to inhibition of peptidoglycan biosynthesis and eventually bacterial lysis due to the inability to synthesize peptidoglycan.

5. Conclusion

In the present study, we searched for genes relevant for CBD susceptibility in *S. aureus* to get a better knowledge on how CBD acts on the cell but also how CBD potentiates the effect of BAC. We identified the *farE/farR* system to be of great interest since multiple mutations were observed in this locus. Furthermore, by screening the Nebraska
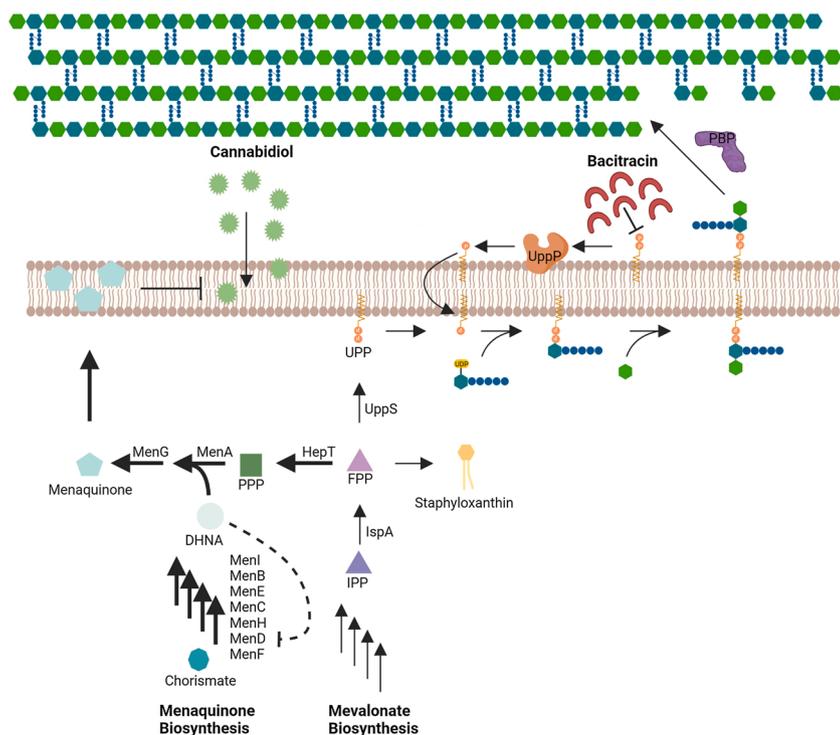
Fig. 5. A proposed model for the CBD mediated potentiation of BAC. BAC interferes with cell wall synthesis by binding to the important lipid carrier undecaprenyl pyrophosphate (UPP) and prevents recycling and further polymerization of the peptidoglycan forcing *de novo* synthesis of UPP by the undecaprenyl pyrophosphate synthase (UppS). Presence of CBD causes membrane potential disruption in *S. aureus* which damaging effect might be prevented by increasing the levels of menaquinone. In combination with BAC, the dephosphorylation of UPP is inhibited increasing the demand for *de novo* synthesis of UPP. Since presence of CBD might cause increased demand for menaquinone and therefore direct the focus of the use of IPP and FPP towards this, the level of UPP produced is low leading to potentiation of BAC. UppP: Undecaprenyl pyrophosphate phosphatase, PBP: Penicillin binding protein, UPP: Undecaprenyl pyrophosphate, UppS: Undecaprenyl pyrophosphate synthase, FPP: Farnesyl pyrophosphate, IPP: Isopentenyl pyrophosphate, PPP: Polyprenyl pyrophosphate and DHNA: 1,4-dihydroxy-2-naphtoic acid. Dashed line indicates a possible DHNA mediated inhibition of MenD. Created using BioRender.com. Publication license can be found in Supplementary F.

Transposon Mutant Library for CBD susceptible strains, we found that the menaquinone pathway to be of great interest. Strains containing deletions of genes encoding enzymes of the menaquinone pathway became more susceptible towards CBD while addition of exogenous menaquinone caused *S. aureus* to become less susceptible towards CBD, highlighting the importance of menaquinone in relation to the activity of CBD and potentially also to the CBD mediated potentiation of BAC. Our observations contribute with several components to the model by which CBD acts as an antimicrobial and as an antibiotic adjuvant to BAC, yet more experiments are needed to fully clarify its mechanism.

6. Author statement

CSW: Conceptualization; Data curation; Formal analysis; Funding acquisition; Investigation; Methodology; Supervision; Validation; Visualization; Roles/Writing - original draft

APR: Investigation

MCL: Investigation

STP: Formal analysis; Writing - review & editing

TK: Formal analysis; Resources; Supervision

MV: Supervision; Writing - review & editing

HI: Supervision; Writing - review & editing

SPP: Funding acquisition; Supervision

JKK: Conceptualization; Funding acquisition; Project administration; Supervision; Roles/Writing - original draft.

Funding

Declaration of Competing Interest

CSW and JKK are listed as inventors on patent applications relating to WO2018234301A1 involving the use of bacitracin and/or daptomycin combined with cannabidiol for treatment of bacterial infections held by University of Southern Denmark.

Acknowledgements

Appendix A. Supplementary data

Supplementary material related to this article can be found, in the online version, at doi:https://doi.org/10.1016/j.micres.2022.126974.

References

Alnaseri, H., Arsic, B., Schneider, J.E., Kaiser, J.C., Scinocca, Z.C., Heinrichs, D.E., McGavin, M.J., 2015. Inducible expression of a resistance-nodulation-Division-Type efflux pump in Staphylococcus aureus provides resistance to linoleic and arachidonic acids. J. Bacteriol. 197, 1893–1905.

Alnaseri, H., Kuiack, R.C., Ferguson, K.A., Schneider, J.E.T., Heinrichs, D.E., McGavin, M.J., 2019. DNA binding and sensor specificity of FarR, a novel TetR family regulator required for induction of the fatty acid efflux pump FarE in Staphylococcus aureus. J. Bacteriol. 201.

Appendino, G., Gibbons, S., Giana, A., Pagani, A., Grassi, G., Stavri, M., Smith, E., Rahman, M., 2008. Antibacterial cannabinoids from Cannabis sativa: a structure-activity study. J. Nat. Prod. 71, 1427–1430.

Aslam, B., Wang, W., Arshad, M.I., Khurshid, M., Muzammil, S., Rasool, M.H., Nisar, M. A., Alvi, R.F., Aslam, M.A., Qamar, M.U., Salamat, M.K.F., Baloch, Z., 2018. Antibiotic resistance: a rundown of a global crisis. Infect. Drug Resist. 11, 1645–1658.

Bakker, E.P., Mangerich, W.E., 1981. Interconversion of components of the bacterial proton motive force by electrogenic potassium transport. J. Bacteriol. 147, 820–826.

Balibar, C.J., Shen, X., Tao, J., 2009. The mevalonate pathway of Staphylococcus aureus. J. Bacteriol. 191, 851–861.

Bashiri, G., Nigon, L.V., Jirgis, E.N.M., Ho, N.A.T., Stanborough, T., Dawes, S.S., Baker, E.N., Bulloch, E.M.M., Johnston, J.M., 2020. Allosteric regulation of menaquinone (vitamin K(2)) biosynthesis in the human pathogen Mycobacterium tuberculosis. J. Biol. Chem. 295, 3759–3770.

Bin Zaman, S., Hussain, M.A., Nye, R., Mehta, V., Mamun, K.T., Hossain, N., 2017. A review on antibiotic resistance: alarm bells are ringing. Cureus 9.

Blaskovich, M.A.T., Kavanagh, A.M., Elliott, A.G., Zhang, B., Ramu, S., Amado, M., Lowe, G.J., Hinton, A.O., Pham, D.M.T., Zuegg, J., Beare, N., Quach, D., Sharp, M.D., Pogliano, J., Rogers, A.P., Lyras, D., Tan, L., West, N.P., Crawford, D.W., Peterson, M.L., Callahan, M., Thurn, M., 2021. The antimicrobial potential of cannabidiol. Commun. Biol. 4, 7.

Bosch, M.E., Bertrand, B.P., Heim, C.E., Alqarzaee, A.A., Chaudhari, S.S., Aldrich, A.L., Fey, P.D., Thomas, V.C., Kielian, T., Torres, V.J., 2020. Staphylococcus aureus ATP synthase promotes biofilm persistence by influencing innate immunity. mBio 11, e01581–01520.

Boyle-Vavra, S., Challapalli, M., Daum, R.S., 2003. Resistance to autolysis in vancomycin-selected Staphylococcus aureus isolates precedes vancomycin-intermediate resistance. Antimicrob. Agents Chemother. 47, 2036–2039.

Chen, Y., Moran, J.C., Campbell-Lee, S., Horsburgh, M.J., 2020. Transcriptomic responses and survival mechanisms of staphylococci to the antimicrobial skin lipid sphingosine. bioRxivorg, 2020.2009.2015.297481.

Choi, S.-r., Frandsen, J., Narayanasamy, P., 2017. Novel long-chain compounds with both immunomodulatory and MenA inhibitory activities against Staphylococcus aureus and its biofilm. Sci. Rep. 7, 40077.

Collins, L.V., Kristian, S.A., Weidenmaier, C., Faigle, M., van Kessel, K.P.M., van Strijp, J. A.G., Götz, F., Neumeister, B., Peschel, A., 2002. Staphylococcus aureus strains lacking d-Alanine modifications of teichoic acids are highly susceptible to human neutrophil killing and are virulence attenuated in mice. J. Infect. Dis. 186, 214–219.

Dawson, A., Fyfe, P.K., Gillet, F., Hunter, W.N., 2011. Exploiting the high-resolution crystal structure of Staphylococcus aureus MenH to gain insight into enzyme activity. BMC Struct. Biol. 11, 19.

Deatherage, D.E., Barrick, J.E., 2014. Identification of mutations in laboratory-evolved microbes from next-generation sequencing data using breseq. Methods Mol. Biol. 1151, 165–188.

Delauné, A., Dubrac, S., Blanchet, C., Poupel, O., Mäder, U., Hiron, A., Leduc, A., Fitting, C., Nicolas, P., Cavaillon, J.M., Adib-Conquy, M., Msadek, T., 2012. The WalKR system controls major staphylococcal virulence genes and is involved in triggering the host inflammatory response. Infect. Immun. 80, 3438–3453.

Diep, B.A., Gill, S.R., Chang, R.F., Phan, T.H., Chen, J.H., Davidson, M.G., Lin, F., Lin, J., Carleton, H.A., Mongodin, E.F., Sensabaugh, G.F., Perdreau-Remington, F., 2006. Complete genome sequence of USA300, an epidemic clone of community-acquired meticillin-resistant Staphylococcus aureus. Lancet 367, 731–739.

Douafer, H., Andrieu, V., Phanstiel, O., Brunel, J.M., 2019. Antibiotic adjuvants: make antibiotics great again! J. Med. Chem. 62, 8665–8681.

Dubrac, S., Boneca, I.G., Poupel, O., Msadek, T., 2007. New insights into the WalK/WalR (YycG/YycF) essential signal transduction pathway reveal a major role in controlling cell wall metabolism and biofilm formation in Staphylococcus aureus. J. Bacteriol. 189, 8257–8269.

Farha, M.A., Verschoor, C.P., Bowdish, D., Brown, E.D., 2013. Collapsing the proton motive force to identify synergistic combinations against Staphylococcus aureus. Chem. Biol. 20, 1168–1178.

Farha, M.A., El-Halfawy, O.M., Gale, R.T., MacNair, C.R., Carfrae, L.A., Zhang, X., Jentsch, N.G., Magolan, J., Brown, E.D., 2020. Uncovering the hidden antibiotic potential of Cannabis. ACS Infect. Dis. 6, 338–346.

Fey, P.D., Endres, J.L., Yajjala, V.K., Widhelm, T.J., Boissy, R.J., Bose, J.L., Bayles, K.W., 2013. A genetic resource for rapid and comprehensive phenotype screening of nonessential Staphylococcus aureus genes. mBio 4, e00537–00512.

Friedman, L., Alder, J.D., Silverman, J.A., 2006. Genetic changes that correlate with reduced susceptibility to daptomycin in Staphylococcus aureus. Antimicrob. Agents Chemother. 50, 2137–2145.

Gurung, R.R., Maharjan, P., Chhetri, G.G., 2020. Antibiotic resistance pattern of Staphylococcus aureus with reference to MRSA isolates from pediatric patients. Future Sci. OA 6. Fso464.

Hammer, N.D., Reniere, M.L., Cassat, J.E., Zhang, Y., Hirsch, A.O., Indriati Hood, M., Skaar, E.P., 2013. Two heme-dependent terminal oxidases power Staphylococcus aureus organ-specific colonization of the vertebrate host. mBio 4.

Helle, L., Kull, M., Mayer, S., Marincola, G., Zelder, M.-E., Goerke, C., Wolz, C., Bertram, R., 2011. Vectors for improved Tet repressor-dependent gradual gene induction or silencing in Staphylococcus aureus. Microbiology 157, 3314–3323.

Hiron, A., Falord, M., Valle, J., Débarbouillé, M., Msadek, T., 2011. Bacitracin and nisin resistance in Staphylococcus aureus: a novel pathway involving the BraS/BraR two-component system (SA2417/SA2418) and both the BraD/BraE and VraD/VraE ABC transporters. Mol. Microbiol. 81, 602–622.

Howden, B.P., McEvoy, C.R.E., Allen, D.L., Chua, K., Gao, W., Harrison, P.F., Bell, J., Coombs, G., Bennett-Wood, V., Porter, J.L., Robins-Browne, R., Davies, J.K., Seemann, T., Stinear, T.P., 2011. Evolution of multidrug resistance during Staphylococcus aureus infection involves mutation of the essential two component regulator WalKR. PLoS Pathog. 7, e1002359.

Hu, Q., Peng, H., Rao, X., 2016. Molecular events for promotion of vancomycin resistance in vancomycin intermediate Staphylococcus aureus. Front. Microbiol. 7, 1601.

Huang, D.W., Sherman, B.T., Lempicki, R.A., 2009. Systematic and integrative analysis of large gene lists using DAVID bioinformatics resources. Nat. Protoc. 4, 44–57.

Huang da, W., Sherman, B.T., Lempicki, R.A., 2009. Bioinformatics enrichment tools: paths toward the comprehensive functional analysis of large gene lists. Nucleic Acids Res. 37, 1–13.

Ji, Q., Chen, P.J., Qin, G., Deng, X., Hao, Z., Wawrzak, Z., Yeo, W.-S., Quang, J.W., Cho, H., Luo, G.-Z., Weng, X., You, Q., Luan, C.-H., Yang, X., Bae, T., Yu, K., Jiang, H., He, C., 2016. Structure and mechanism of the essential two-component signal-transduction system WalKR in Staphylococcus aureus. Nat. Commun. 7, 11000.

Kohler, T., Weidenmaier, C., Peschel, A., 2009. Wall teichoic acid protects Staphylococcus aureus against antimicrobial fatty acids from human skin. J. Bacteriol. 191, 4482–4484.

Kossakowska-Zwierucho, M., Kaźmierkiewicz, R., Bielawski, K.P., Nakonieczna, J., 2016. Factors determining Staphylococcus aureus susceptibility to photoantimicrobial chemotherapy: RsbU activity, staphyloxanthin level, and membrane fluidity. Front. Microbiol. 7, 1141.

Kurosu, M., Begari, E., 2010. Vitamin K2 in electron transport system: are enzymes involved in vitamin K2 biosynthesis promising drug targets? Molecules 15, 1531–1553.

Langmead, B., Salzberg, S.L., 2012. Fast gapped-read alignment with Bowtie 2. Nat. Methods 9, 357–359.

Laws, M., Shaaban, A., Rahman, K.M., 2019. Antibiotic resistance breakers: current approaches and future directions. FEMS Microbiol. Rev. 43, 490–516.

Liao, Y., Smyth, G.K., Shi, W., 2014. featureCounts: an efficient general purpose program for assigning sequence reads to genomic features. Bioinformatics 30, 923–930.

Ling, L.L., Schneider, T., Peoples, A.J., Spoering, A.L., Engels, I., Conlon, B.P., Mueller, A., Schäberle, T.F., Hughes, D.E., Epstein, S., Jones, M., Lazarides, L., Steadman, V.A., Cohen, D.R., Felix, C.R., Fetterman, K.A., Millett, W.P., Nitti, A.G., Zullo, A.M., Chen, C., Lewis, K., 2015. A new antibiotic kills pathogens without detectable resistance. Nature 517, 455–459.

Love, M.I., Huber, W., Anders, S., 2014. Moderated estimation of fold change and dispersion for RNA-seq data with DESeq2. Genome Biol. 15, 550.

Lowy, F.D., 2003. Antimicrobial resistance: the example of Staphylococcus aureus. J. Clin. Invest. 111, 1265–1273.

Martins, M., Dastidar, S.G., Fanning, S., Kristiansen, J.E., Molnar, J., Pagès, J.-M., Schelz, Z., Spengler, G., Viveiros, M., Amaral, L., 2008. Potential role of non-antibiotics (helper compounds) in the treatment of multidrug-resistant Gram-negative infections: mechanisms for their direct and indirect activities. Int. J. Antimicrob. Agents 31, 198–208.

Medina, E., Pieper, D.H., 2016. Tackling threats and future problems of multidrug-resistant Bacteria. Curr. Top. Microbiol. Immunol. 398, 3–33.

Meehl, M., Herbert, S., Götz, F., Cheung, A., 2007. Interaction of the GraRS two-component system with the VraFG ABC transporter to support vancomycin-intermediate resistance in Staphylococcus aureus. Antimicrob. Agents Chemother. 51, 2679–2689.

Mi, H., Ebert, D., Muruganujan, A., Mills, C., Albou, L.-P., Mushayamaha, T., Thomas, P.D., 2020. PANTHER version 16: a revised family classification, tree-based classification tool, enhancer regions and extensive API. Nucleic Acids Res. 49, D394–D403.

Mike, L.A., Dutter, B.F., Stauff, D.L., Moore, J.L., Vitko, N.P., Aranmolate, O., Kehl-Fie, T.E., Sullivan, S., Reid, P.R., DuBois, J.L., Richardson, A.R., Caprioli, R.M., Sulikowski, G.A., Skaar, E.P., 2013. Activation of heme biosynthesis by a small molecule that is toxic to fermenting Staphylococcus aureus. Proc. Natl. Acad. Sci. 110, 8206–8211.

Monk, I.R., Shah, I.M., Xu, M., Tan, M.W., Foster, T.J., 2012. Transforming the untransformable: application of direct transformation to manipulate genetically Staphylococcus aureus and Staphylococcus epidermidis. mBio 3.

Nguyen, M.-T., Saising, J., Tribelli, P.M., Nega, M., Diene, S.M., François, P., Schrenzel, J., Spröer, C., Bunk, B., Ebner, P., Hertlein, T., Kumari, N., Härtner, T., Wistuba, D., Voravuthikunchai, S.P., Mäder, U., Ohlsen, K., Götz, F., 2019. Inactivation of farR causes high rhodomyrtone resistance and increased pathogenicity in Staphylococcus aureus. Front. Microbiol. 10.

O'Neill, A.J., Chopra, I., 2004. Preclinical evaluation of novel antibacterial agents by microbiological and molecular techniques. Expert Opin. Investig. Drugs 13, 1045–1063.

Pader, V., Hakim, S., Painter, K.L., Wigneshweraraj, S., Clarke, T.B., Edwards, A.M., 2016. Staphylococcus aureus inactivates daptomycin by releasing membrane phospholipids. Nat. Microbiol. 2, 16194.

Patel, D., Husain, M., Vidaillac, C., Steed, M.E., Rybak, M.J., Seo, S.M., Kaatz, G.W., 2011. Mechanisms of in-vitro-selected daptomycin-non-susceptibility in Staphylococcus aureus. Int. J. Antimicrob. Agents 38, 442–446.

Paudel, A., Hamamoto, H., Panthee, S., Matsumoto, Y., Sekimizu, K., 2020. Large-scale screening and identification of novel pathogenic Staphylococcus aureus genes using a silkworm infection model. J. Infect. Dis. 221, 1795–1804.

Peschel, A., Vuong, C., Otto, M., Götz, F., 2000. The d-Alanine residues ofStaphylococcus aureus teichoic acids alter the susceptibility to vancomycin and the activity of autolytic enzymes. Antimicrob. Agents Chemother. 44, 2845–2847.

Schlag, M., Biswas, R., Krismer, B., Kohler, T., Zoll, S., Yu, W., Schwarz, H., Peschel, A., Götz, F., 2010. Role of staphylococcal wall teichoic acid in targeting the major autolysin Atl. Mol. Microbiol. 75, 864–873.

Schuster, C.F., Wiedemann, D.M., Kirsebom, F.C.M., Santiago, M., Walker, S., Gründling, A., 2020. High-throughput transposon sequencing highlights the cell wall as an important barrier for osmotic stress in methicillin resistant Staphylococcus aureus and underlines a tailored response to different osmotic stressors. Mol. Microbiol. 113, 699–717.

Sen, S., Sirobhushanam, S., Johnson, S.R., Song, Y., Tefft, R., Gatto, C., Wilkinson, B.J., 2016. Growth-environment dependent modulation of Staphylococcus aureus branched-chain to straight-chain fatty acid ratio and incorporation of unsaturated fatty acids. PLoS One 11, e0165300.

Shaaly, A., Kalamorz, F., Gebhard, S., Cook, G.M., 2013. Undecaprenyl pyrophosphate phosphatase confers low-level resistance to bacitracin in Enterococcus faecalis. J. Antimicrob. Chemother. 68, 1583–1593.

Sievert, D.M., Rudrik, J.T., Patel, J.B., McDonald, L.C., Wilkins, M.J., Hageman, J.C., 2008. Vancomycin-resistant Staphylococcus aureus in the United States, 2002-2006. Clin. Infect. Dis. 46, 668–674.

Stauff, D.L., Bagaley, D., Torres, V.J., Joyce, R., Anderson, K.L., Kuechenmeister, L., Dunman, P.M., Skaar, E.P., 2008. Staphylococcus aureus HrtA is an ATPase required for protection against heme toxicity and prevention of a transcriptional heme stress response. J. Bacteriol. 190, 3588–3596.

Suzuki, T., Swoboda, J.G., Campbell, J., Walker, S., Gilmore, M.S., 2011. In vitro antimicrobial activity of wall teichoic acid biosynthesis inhibitors against Staphylococcus aureus isolates. Antimicrob. Agents Chemother. 55, 767–774.

Suzuki, T., Campbell, J., Kim, Y., Swoboda, J.G., Mylonakis, E., Walker, S., Gilmore, M.S., 2012. Wall teichoic acid protects Staphylococcus aureus from inhibition by Congo red and other dyes. J. Antimicrob. Chemother. 67, 2143–2151.

Truglio, J.J., Theis, K., Feng, Y., Gajda, R., Machutta, C., Tonge, P.J., Kisker, C., 2003. Crystal structure of Mycobacterium tuberculosis MenB, a key enzyme in vitamin K2 biosynthesis*. J. Biol. Chem. 278, 42352–42360.

van Dalen, R., Peschel, A., van Sorge, N.M., 2020. Wall teichoic acid in Staphylococcus aureus host interaction. Trends Microbiol. 28, 985–998.

Van Klingeren, B., Ten Ham, M., 1976. Antibacterial activity of delta9-tetrahydrocannabinol and cannabidiol. Antonie Van Leeuwenhoek 42, 9–12.

Vergara-Irigaray, M., Maira-Litrán, T., Merino, N., Pier, G.B., Penadés, J.R., Lasa, I., 2008. Wall teichoic acids are dispensable for anchoring the PNAG exopolysaccharide to the Staphylococcus aureus cell surface. Microbiology (Reading, Engl.) 154, 865–877.

Vestergaard, M., Leng, B., Haaber, J., Bojer, M.S., Vegge, C.S., Ingmer, H., 2016. Genome-wide identification of antimicrobial intrinsic resistance determinants in Staphylococcus aureus. Front. Microbiol. 7, 2018.

Vestergaard, M., Nøhr-Meldgaard, K., Bojer, M.S., Nielsen, C.K., Meyer, R.L., Slavetinsky, C., Peschel, A., Ingmer, H., Baquero, F., Pier, G.B., 2017. Inhibition of the ATP Synthase eliminates the Intrinsic Resistance of <i>Staphylococcus aureus</i> towards Polymyxins. mBio 8, e01114–01117.

Wassmann, C.S., Hojrup, P., Klitgaard, J.K., 2020. Cannabidiol is an effective helper compound in combination with bacitracin to kill Gram-positive bacteria. Sci. Rep. 10, 4112.

Wiegand, I., Hilpert, K., Hancock, R.E., 2008. Agar and broth dilution methods to determine the minimal inhibitory concentration (MIC) of antimicrobial substances. Nat. Protoc. 3, 163–175.

Yin, Y., Chen, H., Li, S., Gao, H., Sun, S., Li, H., Wang, R., Jin, L., Liu, Y., Wang, H., 2019. Daptomycin resistance in methicillin-resistant Staphylococcus aureus is conferred by IS256 insertion in the promoter of mprF along with mutations in mprF and walK. Int. J. Antimicrob. Agents 54, 673–680.

Zhang, P., Wright, J.A., Osman, A.A., Nair, S.P., 2017. An aroD ochre mutation results in a Staphylococcus aureus small colony variant that can undergo phenotypic switching via two alternative mechanisms. Front. Microbiol. 8.

Zheng, L., Yan, M., Fan, F., Ji, Y., 2015. The essential WalK histidine kinase and WalR regulator differentially mediate autolysis of Staphylococcus aureus RN4220. J. Nat. Sci. 1.

Zhu, A., Ibrahim, J.G., Love, M.I., 2018. Heavy-tailed prior distributions for sequence count data: removing the noise and preserving large differences. Bioinformatics 35, 2084–2092.